

MULTI-IRS-AIDED WIDEBAND INTEGRATED SENSING AND COMMUNICATIONS

Tong Wei, Linlong Wu, Kumar Vijay Mishra and M. R. Bhavani Shankar

Interdisciplinary Centre for Security, Reliability and Trust (SnT), University of Luxembourg
email: {tong.wei@, linlong.wu@, kumar.mishra@ext., bhavani.shankar@}uni.lu

ABSTRACT

We propose a novel dual-function radar-communications (DFRC) system that relies on multiple intelligent reflecting surfaces (IRSs) to enhance detection of non-line-of-sight (NLoS) targets. In particular, we consider a wideband OFDM transmit signal for which we jointly design the frequency-dependent beamforming and phase shifts to maximize the average SINR of radar and the minimal communication SINR among all users. We solve the resulting highly nonconvex problem comprising maximin objective function with a difference of convex (DC) constraint through an alternating maximization (AM) framework of alternating direction method of multipliers (ADMM) and Dinkelbach's method. Numerical experiments demonstrate that the proposed method with multiple IRS can achieve 3.3 dB radar SINR enhancement and 0.9 dB minimal communication SINR improvement compared with single IRS scenario.

Index Terms— Dual-function radar-communications, intelligent reflecting surfaces, non-line-of-sight path, wideband beamforming.

1. INTRODUCTION

Intelligent reflecting surface (IRS) consists of many low-cost reflecting elements, each of which is capable to control the phase of the impinging signal, independently, and hence alter the wireless propagation environment [1–4]. Thanks to the passive property, IRS shows the huge potential of large-scale deployment with much lower energy consumption [5, 6]. Based on these advantages, IRS can be integrated into the most of wireless system, such as MIMO radar and MIMO communication, to enhance the quality of service (QoS) and detection performance [7–11].

It is known that the propagation properties of wireless channels can not be adaptively controlled with the conventional communication technologies. Hence, exploiting the ability of intelligent spectrum control, the cost and energy efficient IRS is first deployed in wireless communication system [12–16]. For example, in [12], the wireless channel is decomposed into multiple subchannels, thus each of that can be estimated via multi-round pilot training. Combined with the information of all subchannels, the complete channel state information (CSI) is well constructed. After that, the active and passive beamforming vectors are properly designed. To facilitate the implementation, the more practical model is proposed in [14]. The relationship between the amplitude and phase-shift of IRS is considered to match the statement of reflecting device. To form the directional beam and improve the QoS, it is crucial to obtain the precise location of user. In [15], IRS is integrated into the wireless system to assist the estimation of the user position and orientation.

Noted that the above methods rely on both the line-of-sight (LoS) path and non-line-of-sight (NLoS) path between base-station (BS) and users. Hence, if all the LoS paths are blocked, the performance of these schemes have a severe degradation. Toward this end, IRS

is considered as the proper device which can be used to build the extra LoS paths to guarantee the secure communication. For example, in [17], IRS-aided millimeter wave NLoS communications system is developed and the achievable sum-rate is analyzed. Besides, the principle of NLoS radar system is introduced in [18]. Furthermore, in [19], the NLoS radar surveillance system which assisted by the single IRS is considered. In order to extend the radar coverage region which can not be reached by the direct path, IRS is necessary and deployed in the suitable position where exists the LoS path between IRS and transmitter/receiver.

Recently, IRS has been successfully utilized in dual-functional radar and communication (DFRC) [20] to improve the sensing and communication performance, simultaneously [21–24]. For example, in [21], both the passive and active beamforming are devised for the IRS-aided DFRC to enhance the radar detection performance while ensuring the single-user signal-to-noise ratio (SNR). To overcome the single-user limitation, in [22], IRS is utilized to provide the extra path from dual-function base-station (DFBS) to the multiple users. Meanwhile, the transmit beampattern of DFBS is aligned to the direction of targets and the multi-user interference (MUI) is eliminated to guarantee QoS. However, it is noticed that the IRS actually does not sever for target detection. Toward this end, in [23], an efficient two-stage method is developed in IRS-assisted DFRC via designing the transmit signal and phase-shift matrix. During the first stage, a small portion of the IRS is used to transmit the wide beam for target surveillance while using the rest of the IRS elements for communications. As for target localization, a larger portion of the IRS is utilized and the hierarchical phase-shift matrix is properly designed to synthesize the sharper beam. Noticed that the above DFRC frameworks rely on the single IRS in narrow-band case which limits the performance of sensing and communication.

Different from the previous schemes [21–23], in this paper, we focus on combining multi-IRS with wideband DFRC system. The major contributions of this work is summarized as follows: (1). We utilize multiple IRS to assist a wideband DFRC system while all the line-of-sight (LoS) path is blocked [25]. Meanwhile, a novel optimization problem which aim to maximize the average radar SINR and the minimal communication SINR simultaneously, is formulated; (2). An alternating maximization (AM) based algorithm is devised to tackle the resulting problem; (3). Numerical results are provided to illustrate the effectiveness of the proposed design approach.

Notations: Vectors and matrices are denoted by lower case boldface letter and upper case boldface letter, respectively. $(\cdot)^T$, $(\cdot)^*$ and $(\cdot)^H$ denote denote the operations of transpose, conjugate, and Hermitian transpose, respectively. \mathbf{I}_L denotes the $L \times L$ identity matrix and \otimes is the Kroneker product. Meanwhile, $\text{diag}(\cdot)$ denotes the diagonal matrix and $\text{blkdiag}[\mathbf{A}, \mathbf{B}]$ is the block diagonal matrix which the diagonal block consist of \mathbf{A} and \mathbf{B} , respectively. The operator $\text{vec}(\cdot)$ denotes the vectorization of a matrix. Finally, $\|\cdot\|_2$ and $\|\cdot\|_F$ represent the ℓ_2 -norm and Frobenius-norm, respectively.

2. SIGNAL MODEL

Consider an IRS-assisted wideband DFRC system consisting of single target, Q clutter patches, U single-antenna users, N_t -antenna dual-function base-station (DFBS), N_r radar receive antennas, M IRSs with each IRS comprising N_m reflecting elements. Assume that both the DFBS and radar receiver are NLoS with respect to target and users due to some blockage. The transmit signal of U symbol streams is first emitted to IRSs and then reflected to target and users.

The data symbol is modulated and spread over K subcarriers. At the k -th subcarrier, the orthogonal symbol vector for all user is $\mathbf{s}_k \in \mathbb{C}^{U \times 1}$, $k = 1, \dots, K$, where $\mathbb{E}\{\mathbf{s}_k \mathbf{s}_k^H\} = \mathbf{I}_U$. To overcome beam-squint effect, we utilize the frequency-dependent beamforming $\mathbf{F}_k \in \mathbb{C}^{N_t \times U}$ to process the symbol block \mathbf{s}_k . The complex envelope of the transmitted signal at the k -th subcarrier from n_t -th antenna is

$$x_{n_t}(t) = \sum_{k=1}^K \sum_{u=1}^U \mathbf{F}_k(n_t, u) \mathbf{s}_k(u) \text{rect}(t - u\Delta t) e^{j2\pi f_k t}, \quad (1)$$

where $\mathbf{F}_k(n_t, u)$ denotes the (n_t, u) -th element of the matrix \mathbf{F}_k , $\mathbf{s}_k(u)$ is the u -th element of \mathbf{s}_k , the central frequency k -th subcarrier $f_k = (k-1)\Delta f$ and $\Delta f = 1/\Delta t$ is the subcarrier spacing. Consequently, the $N_t \times 1$ transmitted signal vector is given by

$$\mathbf{x}(t) = [x_1(t), \dots, x_{N_t}(t)]^T \in \mathbb{C}^{N_t \times 1}. \quad (2)$$

The steering vectors of BS, radar receiver and m -th IRS are defined as, respectively,

$$\begin{aligned} \mathbf{a}_t(\theta, f_k) &= [1, e^{-jv(\theta, f_k)}, \dots, e^{-j(N_t-1)v(\theta, f_k)}]^T, \\ \mathbf{a}_r(\theta, f_k) &= [1, e^{-jv(\theta, f_k)}, \dots, e^{-j(N_r-1)v(\theta, f_k)}]^T, \\ \mathbf{b}_m(\theta, f_k) &= [1, e^{-jv(\theta, f_k)}, \dots, e^{-j(N_m-1)v(\theta, f_k)}]^T, \end{aligned}$$

where $m = 1 \dots, M$ and $v(\theta, f_k) = 2\pi(f_k + f_c)(\frac{d \sin(\theta)}{c})$.

The received signal from radar receiver at the k -th subcarrier is

$$\begin{aligned} \mathbf{y}_R(f_k) &= \sum_{m=1}^M \mathbf{D}_{m,k} \mathbf{\Phi}_m \mathbf{B}_{m,k} \mathbf{\Phi}_m \mathbf{G}_{m,k} \mathbf{F}_k \mathbf{s}_k \\ &+ \sum_{m=1}^M \mathbf{D}_{m,k} \mathbf{\Phi}_m \tilde{\mathbf{B}}_{m,k} \mathbf{\Phi}_m \mathbf{G}_{m,k} \mathbf{F}_k \mathbf{s}_k + \mathbf{n}_R(f_k), \end{aligned} \quad (3)$$

where $\mathbf{\Phi}_m = \text{diag}(e^{j\phi_{m,1}}, \dots, e^{j\phi_{m,N_m}})$ denotes the phase-shift matrix of m -th IRS, $\mathbf{G}_{m,k} = \beta_{g,m} \mathbf{b}_m(\hat{\theta}_m, f_k) \mathbf{a}_t^T(\theta_m, f_k)$ is the channel matrix coupling the DFBS and the m -th IRS at k -th subcarrier, $\beta_{g,m}$ is the channel coefficient, θ_m and $\hat{\theta}_m$ denote the angle of departure from DFBS to m -th IRS and m -th IRS to radar receiver, respectively¹, $\mathbf{D}_{m,k} = \beta_{d,m} \mathbf{a}_r(\theta_m, f_k) \mathbf{b}_m^T(\hat{\theta}_m, f_k)$ denotes the channel matrix coupling the m -th IRS and the radar receiver at k -th subcarrier and $\beta_{d,m}$ is the channel coefficient, $\mathbf{B}_{m,k} = \alpha_{0,m} \mathbf{b}_m(\theta_{m,0}, f_k) \mathbf{b}_m^T(\theta_{m,0}, f_k)$ denotes the target response matrix of the m -th IRS at k -th subcarrier, $\alpha_{0,m}$ is the complex parameter related with radar cross section (RCS) and $\theta_{0,m}$ is the angle of target w.r.t m -th IRS, $\tilde{\mathbf{B}}_{m,k} = \sum_{q=1}^Q \alpha_{q,m} \mathbf{b}_m(\theta_{m,q}, f_k) \mathbf{b}_m^T(\theta_{m,q}, f_k)$ denotes the clutters response matrix of m -th IRS at k -th subcarrier, $\alpha_{q,m}$, $q = 1, \dots, Q$ are the complex parameter of clutters and $\theta_{m,q}$

¹Hereafter, all angles of arrival/departure are measured w.r.t the array broadside direction and are positive when moving clockwise.

is the angle of clutter w.r.t m -th IRS, and $\mathbf{n}_R(f_k) \in \mathbb{C}^{N_r \times 1}$ is the noise vector of radar. The output SINR at the radar receiver is

$$\text{SINR}_R = \frac{\sum_{k=1}^K \sum_{m=1}^M \|\mathbf{D}_{m,k} \mathbf{\Phi}_m \mathbf{B}_{m,k} \mathbf{\Phi}_m \mathbf{G}_{m,k} \mathbf{F}_k\|_F^2}{\sum_{k=1}^K \sum_{m=1}^M \|\mathbf{D}_{m,k} \tilde{\mathbf{B}}_{m,k} \mathbf{\Phi}_m \mathbf{G}_{m,k} \mathbf{F}_k\|_F^2 + N_r K \sigma_r^2}. \quad (4)$$

The receive signal of the u -th user at k -th subcarrier is

$$\begin{aligned} y_u(f_k) &= \sum_{m=1}^M [\mathbf{h}_{u,m,k}^T \mathbf{\Phi}_m \mathbf{G}_{m,k} \mathbf{f}_{k,u} \mathbf{s}_k(u) \\ &+ \sum_{i \neq u} \mathbf{h}_{u,m,k}^T \mathbf{\Phi}_m \mathbf{G}_{m,k} \mathbf{f}_{k,i} \mathbf{s}_k(i)] + \mathbf{n}_k(u) \end{aligned} \quad (5)$$

where $\mathbf{h}_{u,m,k} \in \mathbb{C}^{N_m \times 1}$ denotes the channel between the u -th user and the m -th IRS, $\mathbf{f}_{k,u}$ denotes the u -th column of \mathbf{F}_k and $\mathbf{n}_k(u)$ is the noise of u -th user. According to (5), the average SINR at the u -th users is

$$\text{SINR}_u = \frac{\sum_{k=1}^K \sum_{m=1}^M \|\mathbf{h}_{u,m,k}^T \mathbf{\Phi}_m \mathbf{G}_{m,k} \mathbf{F}_k \mathbf{\Lambda}_u\|_2^2}{\sum_{k=1}^K \sum_{m=1}^M \|\mathbf{h}_{u,m,k}^T \mathbf{\Phi}_m \mathbf{G}_{m,k} \mathbf{F}_k \bar{\mathbf{\Lambda}}_u\|_2^2 + UK \sigma_c^2}, \quad (6)$$

where σ_c^2 denotes the communication noise power over all subcarriers.

In DFRC system, the average radar SINR and the minimal communication SINR should be maximized, simultaneously, to improve both the sensing and communication ability. Mathematically, the optimization problem can be formulated as

$$\begin{aligned} &\underset{\mathbf{\Phi}_m, \mathbf{F}_k}{\text{maximize}} \quad \omega_r \text{SINR}_R + \omega_c \min_u \{\text{SINR}_u\} \\ &\text{subject to} \quad \sum_{k=1}^K \|\mathbf{F}_k\|_F^2 \leq P, \\ & \quad \quad \quad |\mathbf{\Phi}_m(i, i)| = 1, \forall i, \forall m, \end{aligned} \quad (7)$$

where P denotes the total transmit power, $\omega_r, \omega_c \in (0, 1]$ are the parameters accounting for the trade-off between sensing and communication. Essentially, this formulation indicates that in the presence of only NLoS path, we aim to design jointly both the dual-function precoding matrices and IRS phases to guarantee a satisfying SINR performance for radar and communication. Specifically, the precoding matrices (i.e., active beamforming) enable the beams to concentrate on the multiple IRS, and the IRS will further build the LoS path to reach the targets and users. Noted that problem (7) is nonconvex due to both the objective function and constraints. Hence, we reformulate problem (7) equivalently as

$$\begin{aligned} &\underset{t, \mathbf{\Phi}_m, \mathbf{F}_k}{\text{maximize}} \quad \omega_r \text{SINR}_R + t \\ &\text{subject to} \quad \omega_c \text{SINR}_u \geq t, \forall u, \\ & \quad \quad \quad \sum_{k=1}^K \|\mathbf{F}_k\|_F^2 \leq P, |\mathbf{\Phi}_m(i, i)| = 1, \forall i, \forall m. \end{aligned} \quad (8)$$

where t denotes the threshold for communication SINR which can be predefined based on the system requirement. To tackle problem (8), an alternating maximization (AM) based approach will be devised in the sequel.

3. OPTIMIZATION METHOD

In this section, we will introduce the alternating maximization (AM) algorithm to solve problem (8). Specifically, we first split problem

Algorithm 1 Dinkelbach-based solver for (10)

Input: $t, \zeta_1, \mathbf{Y}_t, \mathbf{Y}_c, \mathbf{R}_u$ and $\bar{\mathbf{R}}_u$

Output: $\mathbf{f}^* = \mathbf{f}_r$.

- 1: Set $r = 0, \mu_r = 0$
 - 2: **repeat**
 - 3: Find the optimal solution \mathbf{f} of (10) with reformulated objective function by CVX
 - 4: Calculate the value:
 $F(\mu_r) = 2\Re(\mathbf{f}_r^H \mathbf{Y}_t \mathbf{f}) - \mu_r(\mathbf{f}^H \mathbf{Y}_c \mathbf{f} + N_r K \sigma_r^2)$.
 - 5: Update $\mu_r = 2\Re(\mathbf{f}_r^H \mathbf{Y}_t \mathbf{f}) / (\mathbf{f}^H \mathbf{Y}_c \mathbf{f} + N_r K \sigma_r^2)$
 - 6: Set $r \leftarrow r + 1$
 - 7: **until**
 $F(\mu_r) \leq \zeta_1$ or maximum iteration time reached
-

(8) into three subproblems. Then, at each iteration, the corresponding subproblems are tackled iteratively.

1. *Update of precoding matrices* \mathbf{F}_k

For the given t and Φ_m , the optimization problem corresponding with \mathbf{F}_k is given by

$$\begin{aligned} & \underset{\mathbf{F}_k}{\text{maximize}} \frac{\sum_{k=1}^K \sum_{m=1}^M \|\mathbf{D}_{m,k} \Phi_m \mathbf{B}_{m,k} \Phi_m \mathbf{G}_{m,k} \mathbf{F}_k\|_F^2}{\sum_{k=1}^K \sum_{m=1}^M \|\mathbf{D}_{m,k} \Phi_m \tilde{\mathbf{B}}_{m,k} \Phi_m \mathbf{G}_{m,k} \mathbf{F}_k\|_F^2 + N_r K \sigma_r^2} \\ & \text{subject to} \frac{\sum_{k=1}^K \sum_{m=1}^M \|\mathbf{h}_{u,m,k}^T \Phi_m \mathbf{G}_{m,k} \mathbf{F}_k \boldsymbol{\Lambda}_u\|_2^2}{\sum_{k=1}^K \sum_{m=1}^M \|\mathbf{h}_{u,m,k}^T \Phi_m \mathbf{G}_{m,k} \mathbf{F}_k \bar{\boldsymbol{\Lambda}}_u\|_2^2 + UK \sigma_c^2} \geq \frac{t}{\omega_c}, \\ & \forall u, \|\mathbf{F}_k\|_F^2 \leq P, \end{aligned} \quad (9)$$

which is nonconvex due to the fractional objective function and difference of convex (DC) constraint. Hence, we can simplify problem as

$$\begin{aligned} & \underset{\mathbf{f}}{\text{maximize}} \frac{\mathbf{f}^H \mathbf{Y}_t \mathbf{f}}{\mathbf{f}^H \mathbf{Y}_c \mathbf{f} + N_r K \sigma_r^2} \\ & \text{subject to} \frac{t}{\omega_c} \mathbf{f}^H \bar{\mathbf{R}}_u \mathbf{f} - 2\Re\{\mathbf{f}_n^H \mathbf{R}_u \mathbf{f}\} \leq -\frac{tUK\sigma_c^2}{\omega_c}, \forall u, \\ & \|\mathbf{f}\|_2^2 \leq P, \end{aligned} \quad (10)$$

where $\mathbf{f} = [\text{vec}(\mathbf{F}_1)^T, \dots, \text{vec}(\mathbf{F}_K)^T]^T$ denotes the precoding vector for all subcarriers, $\mathbf{Y}_t = \text{blkdiag}[\mathbf{Y}_1^{(t)}, \dots, \mathbf{Y}_K^{(t)}]$, $\mathbf{Y}_c = \text{blkdiag}[\mathbf{Y}_1^{(c)}, \dots, \mathbf{Y}_K^{(c)}]$, $\mathbf{R}_u = \text{blkdiag}[\mathbf{R}_1^{(u)}, \dots, \mathbf{R}_K^{(u)}]$, $\bar{\mathbf{R}}_u = \text{blkdiag}[\bar{\mathbf{R}}_1^{(u)}, \dots, \bar{\mathbf{R}}_K^{(u)}]$ denote the fixed-value matrices for radar SINR and communication SINR, respectively, and

$$\begin{aligned} \mathbf{Y}_{m,k}^{(t)} &= \mathbf{G}_{m,k} \Phi_{m,k} \mathbf{B}_{m,k} \Phi_{m,k}^H \mathbf{D}_{m,k}, \\ \mathbf{Y}_{m,k}^{(c)} &= \mathbf{G}_{m,k} \Phi_{m,k} \tilde{\mathbf{B}}_{m,k} \Phi_{m,k}^H \mathbf{D}_{m,k}, \\ \mathbf{Y}_k^{(t)} &= \sum_{m=1}^M (\mathbf{I}_U \otimes \mathbf{Y}_{m,k}^{(t)})^H (\mathbf{I}_U \otimes \mathbf{Y}_{m,k}^{(t)}), \\ \mathbf{Y}_k^{(c)} &= \sum_{m=1}^M (\mathbf{I}_U \otimes \mathbf{Y}_{m,k}^{(c)})^H (\mathbf{I}_U \otimes \mathbf{Y}_{m,k}^{(c)}), \\ \mathbf{R}_k^{(u)} &= \sum_{m=1}^M (\boldsymbol{\Lambda}_u \otimes \mathbf{G}_{m,k}^H \mathbf{H}_{u,m,k}^H \phi_m^* \phi_m^T \mathbf{H}_{u,m,k} \mathbf{G}_{m,k}), \\ \bar{\mathbf{R}}_k^{(u)} &= \sum_{m=1}^M (\bar{\boldsymbol{\Lambda}}_u \otimes \mathbf{G}_{m,k}^H \mathbf{H}_{u,m,k}^H \phi_m^* \phi_m^T \mathbf{H}_{u,m,k} \mathbf{G}_{m,k}). \end{aligned}$$

Since problem (10) is the fractional programming with a convex feasible set, it can be solved by the Dinkelbach-based algorithm [26]. Algorithm 1 summarizes this solving method to problem (10).

2. *Update of phase-shift* Φ_m

For the given t and \mathbf{F}_k , the optimization problem corresponding with Φ_m is given by

$$\begin{aligned} & \underset{\Phi_m}{\text{maximize}} \frac{\sum_{k=1}^K \sum_{m=1}^M \|\mathbf{D}_{m,k} \Phi_m \mathbf{B}_{m,k} \Phi_m \mathbf{G}_{m,k} \mathbf{F}_k\|_F^2}{\sum_{k=1}^K \sum_{m=1}^M \|\mathbf{D}_{m,k} \Phi_m \tilde{\mathbf{B}}_{m,k} \Phi_m \mathbf{G}_{m,k} \mathbf{F}_k\|_F^2 + N_r K \sigma_r^2} \\ & \text{subject to} |\Phi_m| = 1, \\ & \frac{\sum_{k=1}^K \sum_{m=1}^M \|\mathbf{h}_{u,m,k}^T \Phi_m \mathbf{G}_{m,k} \mathbf{F}_k \boldsymbol{\Lambda}_u\|_2^2}{\sum_{k=1}^K \sum_{m=1}^M \|\mathbf{h}_{u,m,k}^T \Phi_m \mathbf{G}_{m,k} \mathbf{F}_k \bar{\boldsymbol{\Lambda}}_u\|_2^2 + UK \sigma_c^2} \geq \frac{t}{\omega_c}, \forall u, \end{aligned} \quad (11)$$

which is highly nonconvex due to the quartic fractional objective function and DC constraints. Hence, we introduce the variable ψ to reformulate the problem as

$$\begin{aligned} & \underset{\phi, \psi}{\text{maximize}} \quad f(\phi, \psi) := \frac{\phi^H \Xi_t \phi}{\phi^H \Xi_c \phi} = \frac{\psi^H \Sigma_t \psi}{\psi^H \Sigma_c \psi} \\ & \text{subject to} \quad |\phi| = 1, |\psi| = 1, \phi = \psi \\ & \frac{\phi^H \mathbf{E}_u \phi}{\phi^H \hat{\mathbf{E}}_u \phi} \geq \frac{t}{\omega_c}, \forall u, \end{aligned} \quad (12)$$

where $\phi_m = \Phi_m \mathbf{1}$, $\phi = [\phi_1^T, \dots, \phi_M^T]^T$,

$$\mathbf{E}_m^{(u)} = \sum_{k=1}^K \mathbf{H}_{u,m,k} \mathbf{G}_{m,k} \mathbf{F}_k \boldsymbol{\Lambda}_u \mathbf{F}_k^H \mathbf{G}_{m,k}^H \mathbf{H}_{u,m,k}^H,$$

$$\hat{\mathbf{E}}_m^{(u)} = \sum_{k=1}^K \mathbf{H}_{u,m,k} \mathbf{G}_{m,k} \mathbf{F}_k \bar{\boldsymbol{\Lambda}}_u \mathbf{F}_k^H \mathbf{G}_{m,k}^H \mathbf{H}_{u,m,k}^H,$$

$$\Xi_m^{(t)} = \sum_{k=1}^K \mathbf{D}_{m,k}^H \mathbf{D}_{m,k} \odot \mathbf{B}_{m,k}^* \phi_m^* \mathbf{G}_{m,k}^* \mathbf{F}_k^* \mathbf{F}_k^T \mathbf{G}_{m,k}^T \phi_m^T \mathbf{B}_{m,k}^T,$$

$$\Xi_m^{(c)} = \sum_{k=1}^K \mathbf{D}_{m,k}^H \mathbf{D}_{m,k} \odot \tilde{\mathbf{B}}_{m,k}^* \phi_m^* \mathbf{G}_{m,k}^* \mathbf{F}_k^* \mathbf{F}_k^T \mathbf{G}_{m,k}^T \phi_m^T \tilde{\mathbf{B}}_{m,k}^T,$$

$$\Sigma_m^{(t)} = \sum_{k=1}^K \mathbf{B}_{m,k}^H \phi_m^H \mathbf{D}_{m,k}^H \mathbf{D}_{m,k} \phi_m \mathbf{B}_{m,k} \odot \mathbf{G}_{m,k}^* \mathbf{F}_k^* \mathbf{F}_k^T \mathbf{G}_{m,k}^T,$$

$$\Sigma_m^{(c)} = \sum_{k=1}^K \tilde{\mathbf{B}}_{m,k}^H \phi_m^H \mathbf{D}_{m,k}^H \mathbf{D}_{m,k} \phi_m \tilde{\mathbf{B}}_{m,k} \odot \mathbf{G}_{m,k}^* \mathbf{F}_k^* \mathbf{F}_k^T \mathbf{G}_{m,k}^T,$$

$$\mathbf{E}_u = \text{blkdiag}[\mathbf{E}_1^{(u)}, \dots, \mathbf{E}_M^{(u)}], \hat{\mathbf{E}}_u = \text{blkdiag}[\hat{\mathbf{E}}_1^{(u)}, \dots, \hat{\mathbf{E}}_M^{(u)}],$$

$$\Xi_{t,c} = \text{blkdiag}[\Xi_1^{(t,c)}, \dots, \Xi_M^{(t,c)}],$$

$$\Sigma_{t,c} = \text{blkdiag}[\Sigma_1^{(t,c)}, \dots, \Sigma_M^{(t,c)}].$$

Problem (12) consists of multi-variable fractional quadratic objective function and DC constraint. Hence, we can combine the Dinkelbach method and ADMM to tackle problem (12). First, the objective function of (12) can be reformulated as

$$\begin{aligned} \hat{f}(\lambda, \phi, \psi) &= \phi^H \Xi_t \phi - \lambda \phi^H \Xi_c \phi \\ &= \psi^H \Sigma_t \psi - \lambda \psi^H \Sigma_c \psi. \end{aligned} \quad (13)$$

Then, the augmented Lagrangian function associated with (12) is given by

$$\begin{aligned} \mathcal{L}(\lambda, \phi, \psi, \mathbf{u}, \mathbf{v}) &= \hat{f}(\lambda, \phi, \psi) - \frac{\rho_1}{2} \|\phi - \psi + \mathbf{u}\|_2^2 \\ &\quad - \frac{\rho_2}{2} \sum_u \left| \frac{t}{\omega_c} \phi^H \hat{\mathbf{E}}_u \phi - \phi^H \mathbf{E}_u \phi + v_u \right|_2^2 + \text{const}. \end{aligned} \quad (14)$$

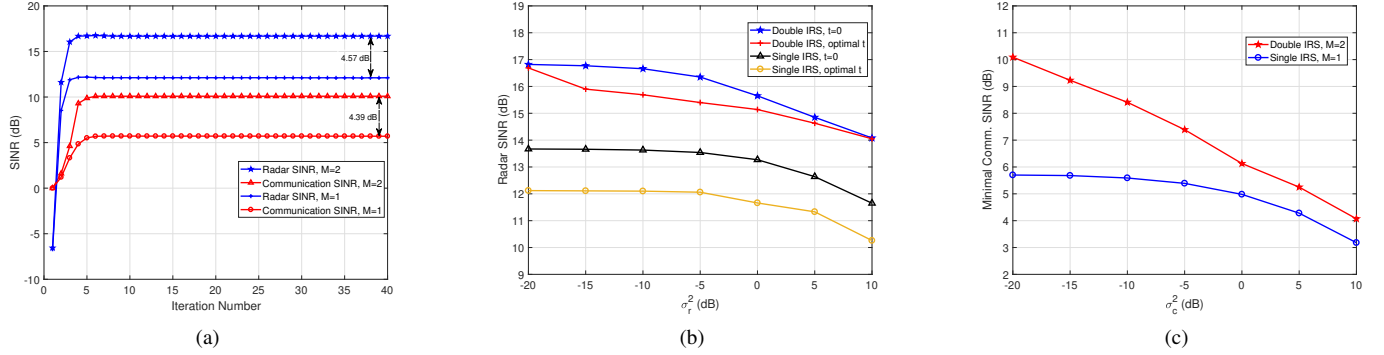


Fig. 1. (a) Objective value versus number of iterations. (b) Radar SINR versus radar noise power σ_r^2 (c) Minimal communication SINR versus communication noise power σ_c^2

where \mathbf{u} and $\mathbf{v} \succeq \mathbf{0}$ denote the dual variables, and $const.$ represent an unrelated constant term. We utilize the first-order Taylor expansion to linearize the convex part of the augmented Lagrangian function (14). Based on above, ADMM-based update formulas are given by

$$\lambda^{(t+1)} = f(\lambda^{(t)}, \phi^{(t)}, \psi^{(t)}) \quad (15a)$$

$$\phi^{(t+1)} = \arg \max_{|\phi|=1} \hat{\mathcal{L}}(\lambda^{(t+1)}, \phi, \psi^{(t)}, \mathbf{u}^{(t)}, \mathbf{v}^{(t)}), \quad (15b)$$

$$\psi^{(t+1)} = \arg \max_{|\psi|=1} \hat{\mathcal{L}}(\lambda^{(t+1)}, \phi^{(t+1)}, \psi, \mathbf{u}^{(t)}, \mathbf{v}^{(t)}), \quad (15c)$$

$$\mathbf{u}^{(t+1)} = \mathbf{u}^{(t)} + \rho_1(\phi^{(t+1)} - \psi^{(t+1)}), \quad (15d)$$

$$\mathbf{v}^{(t+1)} = \mathbf{v}^{(t)} - \rho_2 \left(\frac{t}{\omega_c} \phi^{(t)H} \hat{\mathbf{E}}_u \phi^{(t)} - \phi^{(t)H} \mathbf{E}_u \phi^{(t)} \right). \quad (15e)$$

At each iteration of ADMM, the subproblems w.r.t phase-shift Φ_m and Ψ_m are solved by Riemannian steepest decent (RSD) algorithm [22]. Due to the limited space, the RSD algorithm will be illustrated with details in the full version of this work.

3. Update of auxiliary variable t

For the given \mathbf{F}_k and Φ_m , the problem with respect to t is

$$\begin{aligned} & \text{maximize } t \\ & \text{subject to } \text{SINR}_u \geq \frac{t}{\omega_c}, \forall u. \end{aligned} \quad (16)$$

We can update it by

$$t = \max\{t_n, \arg \min_u \omega_c \text{SINR}_u\}, \quad (17)$$

where t_n denotes the value of t at the last iteration. Note that (17) guarantees that t is the monotonically nondecreasing with the iterations.

4. NUMERICAL EXPERIMENTS

In the simulations, both the DFBS and radar receiver are equipped with the ULA with $N_t = 4$ and $N_r = 4$ elements, respectively. Two IRSs locating at -45° and 45° are used to assist the DFRC system, each of which consists of $N_m = 15$ reflecting elements. The central frequency is 10 GHz and the subcarrier step-size is set as 20 MHz. Meanwhile, we set $K = 32$ and $U = 2$, respectively. The diagonal matrices $\Phi_m, m = 1, 2$, are initialized with the diagonal entries generated from a zero-mean Gaussian distribution. The matrices $\mathbf{F}_k, k = 1, \dots, K$ are initialized with all elements being one.

Meanwhile, we set the trade-off parameters $\omega_r = 1$ and $\omega_c = 1$. The maximum iteration for both inner-loop and out-loop are set as 50 times.

Fig. 1(a) shows the achievable SINR versus the number of iterations for different number of RIS M . It can be seen that the propose algorithm converges within around 10 iterations. Comparing to the single IRS case (i.e. $M = 1$), the double IRS scenario (i.e. $M = 2$) is superior with about 4.5 dB extra gain for both the radar and minimal communication SINR.

Fig. 1(b) demonstrates the achieved radar SINR versus radar noise power. Note that when $t = 0$, the first constraint in problem (8) vanishes, and thereby, the model reduces into a radar-only system. We can observe that the achieved radar SINR decreases when the radar noise power increases. In general, the radar-only system can obtain a higher SINR compared with DFRC system. Meanwhile, the double-IRS assisted DFRC can achieve at least 3.3 dB SINR enhancement compared with the single-IRS case in different noise level.

Fig. 1(c) shows the achieved minimal communication SINR versus the user noise power. It is seen that the communication SINR is reduced as the increasing communication noise power. In addition, the double-IRS assisted DFRC can also achieve at least 0.9 dB communication SINR improvement compared with the single-IRS case in different noise power.

5. SUMMARY

In this paper, we consider use the multiple IRS to assist the wideband dual-function radar communication system which does not exist the LoS path from transmitter to target/user. Specifically, we aim to design the precoding and phase-shift matrices to improve the radar SINR and the minimal communication SINR among all users, simultaneously. However, the resulting optimization problem which consists of maximin objective function, constant-modulus and DC constraint, is highly nonconvex. Toward this end, we develop the AM algorithm which combines both ADMM and Dinkelbach's method to solves the corresponding subproblems. Simulation results demonstrate the efficacy of our approach and the improved SINR performance.

Acknowledgment

This work was supported by the Luxembourg National Research Fund (FNR) through the SPRINGER Project, ref 12734677.

6. REFERENCES

- [1] M. Di Renzo, A. Zappone, M. Debbah, M.-S. Alouini, C. Yuen, J. de Rosny, and S. Tretyakov, "Smart radio environments empowered by reconfigurable intelligent surfaces: How it works, state of research, and the road ahead," *IEEE Journal on Selected Areas in Communications*, vol. 38, no. 11, pp. 2450–2525, 2020.
- [2] Q. Wu and R. Zhang, "Towards smart and reconfigurable environment: Intelligent reflecting surface aided wireless network," *IEEE Communications Magazine*, vol. 58, no. 1, pp. 106–112, 2020.
- [3] O. Özdogan, E. Björnson, and E. G. Larsson, "Intelligent reflecting surfaces: Physics, propagation, and pathloss modeling," *IEEE Wireless Communications Letters*, vol. 9, no. 5, pp. 581–585, 2020.
- [4] J. A. Hodge, K. V. Mishra, and A. I. Zaghoul, "Intelligent time-varying metasurface transceiver for index modulation in 6G wireless networks," *IEEE Antennas and Wireless Propagation Letters*, vol. 19, no. 11, pp. 1891–1895, 2020.
- [5] Q. Wu and R. Zhang, "Intelligent reflecting surface enhanced wireless network via joint active and passive beamforming," *IEEE Transactions on Wireless Communications*, vol. 18, no. 11, pp. 5394–5409, 2019.
- [6] C. Huang, A. Zappone, G. C. Alexandropoulos, M. Debbah, and C. Yuen, "Reconfigurable intelligent surfaces for energy efficiency in wireless communication," *IEEE Transactions on Wireless Communications*, vol. 18, no. 8, pp. 4157–4170, 2019.
- [7] S. Buzzi, E. Grossi, M. Lops, and L. Venturino, "Radar target detection aided by reconfigurable intelligent surfaces," *IEEE Signal Processing Letters*, vol. 28, pp. 1315–1319, 2021.
- [8] W. Lu, B. Deng, Q. Fang, X. Wen, and S. Peng, "Intelligent reflecting surface-enhanced target detection in mimo radar," *IEEE Sensors Letters*, vol. 5, no. 2, pp. 1–4, 2021.
- [9] S. Buzzi, E. Grossi, M. Lops, and L. Venturino, "Radar target detection aided by reconfigurable intelligent surfaces," *IEEE Signal Processing Letters*, vol. 28, pp. 1315–1319, 2021.
- [10] C. Pan, H. Ren, K. Wang, W. Xu, M. ElKashlan, A. Nallanathan, and L. Hanzo, "Multicell mimo communications relying on intelligent reflecting surfaces," *IEEE Transactions on Wireless Communications*, vol. 19, no. 8, pp. 5218–5233, 2020.
- [11] Z. Li, M. Hua, Q. Wang, and Q. Song, "Weighted sum-rate maximization for multi-irs aided cooperative transmission," *IEEE Wireless Communications Letters*, vol. 9, no. 10, pp. 1620–1624, 2020.
- [12] Z. Zhou, N. Ge, Z. Wang, and L. Hanzo, "Joint transmit precoding and reconfigurable intelligent surface phase adjustment: A decomposition-aided channel estimation approach," *IEEE Transactions on Communications*, vol. 69, no. 2, pp. 1228–1243, 2021.
- [13] J. Liu, X. Qian, and M. Di Renzo, "Interference analysis in reconfigurable intelligent surface-assisted multiple-input multiple-output systems," in *ICASSP 2021 - 2021 IEEE International Conference on Acoustics, Speech and Signal Processing (ICASSP)*, 2021, pp. 8067–8071.
- [14] S. Abeywickrama, R. Zhang, Q. Wu, and C. Yuen, "Intelligent reflecting surface: Practical phase shift model and beamforming optimization," *IEEE Transactions on Communications*, vol. 68, no. 9, pp. 5849–5863, 2020.
- [15] A. Elzanaty, A. Guerra, F. Guidi, and M.-S. Alouini, "Reconfigurable intelligent surfaces for localization: Position and orientation error bounds," *IEEE Transactions on Signal Processing*, vol. 69, pp. 5386–5402, 2021.
- [16] M. F. Ahmed, K. P. Rajput, N. K. Venkatesowda, K. V. Mishra, and A. K. Jagannatham, "Joint transmit and reflective beamformer design for secure estimation in IRS-aided WSNs," *arXiv preprint arXiv:2201.04278*, 2022.
- [17] S. N. Sur, A. K. Singh, D. Kandar, and R. Bera, "Sum-rate analysis of intelligent reflecting surface aided multi-user millimeter wave communications system," *Journal of Physics: Conference Series*, vol. 1921, no. 1, p. 012050, may 2021.
- [18] B. Watson and J. R. Guerri, "Non-line-of-sight radar," *Artech House*, 2019.
- [19] A. Aubry, A. De Maio, and M. Rosamilia, "Reconfigurable intelligent surfaces for n-los radar surveillance," *IEEE Transactions on Vehicular Technology*, vol. 70, no. 10, pp. 10 735–10 749, 2021.
- [20] K. V. Mishra, M. B. Shankar, V. Koivunen, B. Ottersten, and S. A. Vorobyov, "Toward millimeter-wave joint radar communications: A signal processing perspective," *IEEE Signal Processing Magazine*, vol. 36, no. 5, pp. 100–114, 2019.
- [21] Z.-M. Jiang, M. Rihan, P. Zhang, L. Huang, Q. Deng, J. Zhang, and E. M. Mohamed, "Intelligent reflecting surface aided dual-function radar and communication system," *IEEE Systems Journal*, pp. 1–12, 2021.
- [22] X. Wang, Z. Fei, Z. Zheng, and J. Guo, "Joint waveform design and passive beamforming for ris-assisted dual-functional radar-communication system," *IEEE Transactions on Vehicular Technology*, vol. 70, no. 5, pp. 5131–5136, 2021.
- [23] R. S. P. Sankar, B. Deepak, and S. P. Chepuri, "Joint communication and radar sensing with reconfigurable intelligent surfaces," *arXiv*, 2021.
- [24] K. V. Mishra, A. Chattopadhyay, S. S. Acharjee, and A. P. Petropulu, "OptM3Sec: Optimizing multicast IRS-aided multi-antenna DFRC secrecy channel with multiple eavesdroppers," in *IEEE International Conference on Acoustics, Speech and Signal Processing*, 2021, in press.
- [25] Z. Esmailbeig, K. V. Mishra, and M. Soltanalian, "IRS-aided radar: Enhanced target parameter estimation via intelligent reflecting surfaces," *arXiv preprint arXiv:2110.13251*, 2021.
- [26] D. W., "On nonlinear fractional programming," *Management Science*, vol. 13, no. 7, pp. 492–498, 1967.